2011 American Control Conference
on O'Farrell Street, San Francisco, CA, USA
June 29 - July 01, 2011

LPV Identification of High Performance Positioning Devices

Roland Tóth, Marc van de Wal, Peter S. C. Heuberger and Paul M. J. Van den Hof

Abstract— **High performance positioning devices exhibit position dependent dynamics in the form of varying flexible modes, which are expected to dominate the dynamic behavior in the new generation of lightweight positioning structures. To handle such position-dependent behavior, the framework of Linear Parameter-Varying (LPV) systems offers powerful tools in terms of control synthesis with many successful practical applications. However, to achieve the desired performance, a low complexity but accurate LPV model of the underlying plant is of crucial importance. Obtaining LPV models for positioning devices based on first principle laws is a rigorous and costly process often resulting in models with inadequate accuracy. Therefore a data driven-modeling approach using Orthonormal Basis Functions (OBF's) is studied for the control-oriented modeling of xy-positioning table dynamics. Through a simulation study it is demonstrated that the proposed modeling procedure, using only measurement data, can provide models whose accuracy is very close to the analytic models derived with the full knowledge of the system.**

I. INTRODUCTION

High performance positioning devices, such as component mounters, xy-positioning tables, and electromagnetic levitation systems, are mechatronic machines with a high demand of accurate servo control. As a common feature of many electromechanical servo systems, the linearized (or so called local) dynamics of these devices varies with the actual position of the device, often manifesting in terms of position-dependent resonant dynamics. For instance, resonance frequencies (poles) may change due to a position-dependent mass matrix (as for the practical case in this paper) or anti-resonances (zeros) may change due to observing mode shapes differently at different positions. Flexible phenomena in general introduce practical limitations on the achievable bandwidth (see, e.g., [1]), which is even more serious in case they are position-dependent. To deal with such phenomena, common control design strategies aim at the synthesis of a sufficiently robust *linear time-invariant* (LTI) controller to accommodate for the variations of the local dynamical behavior of the plant around various positions/operating conditions. This is usually accomplished by identifying *frequency response functions* (FRFs) of the plant for a set of positions and using these responses to design the robust controller with either manual SISO loop-shaping or with more advanced robust synthesis approaches based on $\mathcal{H}_\infty$-optimization or μ-synthesis (see e.g., [2]–[4]). However, all mentioned approaches have in common that the position-dependent dynamics are dealt with by means of robustness, possibly causing conservatism with (strong) limitations on the achievable performance. Furthermore, due to the tightening specifications current developments of positioning devices point to the direction of lightweight structures that typically have their flexible modes occurring at lower frequencies, while also the number of critical modes in the frequency range of interest increases. This in combination with the ever increasing demands on position accuracy and servo bandwidth gives rise to the prediction that position-dependent flexible dynamics will be highly relevant in the dynamic analysis and control design of the future generation of high performance positioning devices. This gives that the currently used synthesis methods will be too conservative.

The framework of *linear parameter-varying* (LPV) systems has been established to efficiently handle position-dependent nonlinear or time-varying dynamics. In LPV systems the signal relations are considered to be linear just as in the LTI case, but the parameters are assumed to be functions of a measurable time-varying signal, the so-called *scheduling variable* $p : \mathbb{Z} \to \mathbb{P}$. The compact set $\mathbb{P} \subset \mathbb{R}^{n_\mathbb{P}}$ denotes the so called *scheduling space*. The LPV system class has a wide representation capability of physical processes and this framework is also supported by a well-worked-out control theory (see, [5]–[7]) with many successful applications. Therefore the LPV framework offers an attractive candidate to provide servo control of positioning devices on a higher bandwidth than what current solutions are capable of. However, to achieve the desired performance, a low complexity but accurate LPV model of the underlying plant is of crucial importance. In general, obtaining LPV models based on first-principle laws is a rigorous and costly process and is expected to be very difficult for lightweight structures. Thus for such devices it may be more attractive to derive models based on measured data.

In the past, there have been some attempts to apply LPV control on positioning devices (e.g., [8]). However, due to the immature state of data-driven LPV modeling, or so called *identification*, the lack of an efficient LPV model prevented to show a significant performance increase with LPV servo control. Due to recent advances of the LPV identification literature (for an overview see [9], [10]), it has become possible to obtain low complexity but accurate models of positioning structures based entirely on measured data. In the current paper, we aim to investigate the current possibilities of LPV identification of high-performance positioning devices through a simulation example of an xy-

The support of Philips Apptech and the Netherlands Organization for Scientific Research (NWO) (grant no. 680-50-0927) is gratefully acknowledged. R. Tóth, P.S.C. Heuberger and P.M.J. Van den Hof are with Delft Center for Systems and Control, Delft University of Technology, Mekelweg 2, 2628 CD, Delft, The Netherlands, Email: {r.toth, p.s.c.heuberger, p.m.j.vandenhof}@tudelft.nl.

Marc van de Wal is with Philips Applied Technologies, Department of Mechatronics, High Tech Campus 7, 5656 AE Eindhoven, The Netherlands.

positioning table, used in the mass-production of integrated circuits. In the investigated scenario, we show that both frequency-domain specifications of the modeling in terms of local dynamics and global accuracy of the model can be guaranteed through an *orthonormal basis functions* (OBFs) based LPV identification approach applied in closed loop. This method also leads to a *linear fractional representation* (LFR) of the model ready to be used for control synthesis. In order to simplify the underlying identification problem we will focus on the development of a *discrete-time* (DT) model.

The paper is organized as follows: first in Sec. II the general concepts of LPV models and representations are discussed also motivating why the use of OBF models is attractive in terms of identification. This is followed in Sec. III by a brief overview of modeling xy-positioning tables in the LPV context and setting up the first-principle model of such a system whose identification is addressed in the sequel of the paper. Next in Sec. IV, a local type of OBF based LPV identification approach is introduced and demonstrated on the identification problem of the first-principle xy-positioning table model. This is followed by the validation and assessment of the developed LPV-OBF model in Sec. V. Finally in Sec. VI the conclusion about presented results are drawn.

II. LPV MODELS & REPRESENTATIONS

The dynamic description of a discrete-time LPV system $\mathcal{S}$ can be formalized as a convolution in terms of p and the input $u : \mathbb{Z} \to \mathbb{R}^{n_\mathrm{u}}$:

$$y(k) = \sum_{i=0}^{\infty} H_i(p,k)u(k-i), \tag{1}$$

where $y : \mathbb{Z} \to \mathbb{R}^{n_\mathrm{y}}$ denotes the output of $\mathcal{S}$ and $k \in \mathbb{Z}$ is the discrete time. The coefficients H_i of (1) are matrix functions of p and they define the varying linear dynamical relation between u and y. This description is a series expansion representation of $\mathcal{S}$ in terms of the so called *pulse basis* $\{q^{-i}\}_{i=0}^{\infty}$, where q is the time-shift operator, i.e. $q^{-i}u(k) = u(k-i)$. It can be proven that for an asymptotically stable $\mathcal{S}$, the expansion (1) is convergent [10].

If the functions H_i only depend on the instantaneous value of p, i.e. $H_i(p(k))$, then their functional dependence is called *static*. Otherwise the dependence is called *dynamic* when H_i not only depends on the instantaneous but also on time-shifted values of p. An important property of LPV systems is that for a constant scheduling signal, i.e. $p(k) = \mathrm{p}$ for all $k \in \mathbb{Z}$, (1) is equal to a convolution describing an LTI system as each $H_i(p,k)$ is constant. Thus, LPV systems can be seen to be similar to LTI systems, but their signal behavior is different due to the variation of the H_i parameters. Note that there are many formal definitions of LPV systems based on particular model structures and parameterizations. The convolution form (1) can be seen as their generalization.

Two important of these formulations are LPV *state-space* (SS) representations and LFRs commonly used in the control literature. LPV-SS representations of a given LPV system $\mathcal{S}$, denoted as $\mathfrak{R}_{\mathrm{SS}}(\mathcal{S})$, are often defined under the assumption of static dependence in the form of

$$qx = A(p)x + B(p)u, \tag{2a}$$
$$y = C(p)x + D(p)u, \tag{2b}$$

where $x : \mathbb{Z} \to \mathbb{R}^{n_\mathrm{x}}$ is the state signal and A, B, C, D, with appropriate dimensions, are rational matrix functions of p, nonsingular on $\mathbb{P}$. The LFR of $\mathcal{S}$, denoted by $\mathfrak{R}_{\mathrm{LFR}}(\mathcal{S})$, is defined as

$$\begin{bmatrix} qx \\ z \\ y \end{bmatrix} = \begin{bmatrix} A & B_1 & B_2 \\ C_1 & D_{11} & D_{12} \\ C_2 & D_{21} & D_{22} \end{bmatrix} \begin{bmatrix} x \\ w \\ u \end{bmatrix}, \tag{3a}$$

where $\{A, \ldots, D_{22}\}$ are constant matrices with appropriate dimensions and

$$w(k) = \Delta(p(k))z(k), \tag{3b}$$

with $\Delta : \mathbb{P} \to \mathbb{R}^{n_\mathrm{p} \times n_\mathrm{p}}$ being the function of p. Commonly, Δ has a block diagonal structure containing the elements of p and Δ is assumed to vary in a polytope. Additionally, x, w, z are latent (auxiliary) variables of $\mathfrak{R}_{\mathrm{LFR}}(\mathcal{S})$. The *continuous-time* (CT) equivalent of SS representations and LFRs can also be formulated by simply substituting q with the differential operator $\frac{\mathrm{d}}{\mathrm{d}t}$.

In identification, we aim to estimate a dynamical model of the system based on measured data, which corresponds to the estimation of each H_i in (1). This estimation is formalized in terms of a model structure (an abstraction of (1)) and an identification criterion. A particularly attractive model structure in the LPV case follows by the truncation of (1) to a finite number of expansion terms. Assuming static dependence of H_i, the resulting model reads as

$$y(k) = \sum_{i=0}^{n} H_i(p(k))u(k-i), \tag{4}$$

which can be seen as the LPV version of the well known LTI *finite impulse response* (FIR) models. Such models have many attractive properties in terms of identification in opposite to the rather challenging problem of identification of (2a-b) or (3a-b). An important property of (4) is linearity-in-the-coefficients that allows to use linear regression for the estimation of $\{H_i\}_{i=1}^{n}$ as a function of $p(k)$ if they are linearly parameterized:

$$H_i(p(k)) = \sum_{j=0}^{n_i} \theta_{ij} f_{ij}(p(k)), \tag{5}$$

where $\theta_{ij} \in \mathbb{R}^{n_\mathrm{Y} \times n_\mathrm{U}}$ are the unknown parameters and f_{ij} are prior selected functions. Furthermore, noise or disturbances in the system can be modeled in an *output error* (OE) sense with this model structure, which allows independent parametrization of the noise model. However, a well known disadvantage of FIR models, both in the LTI and the LPV cases, is that the expansion may have a slow convergence rate, meaning that it requires a relatively large number of parameters for an adequate approximation of the system. In order to benefit from the same properties, but achieve faster convergence rate of the expansion, it is attractive to use basis functions which, opposite to q^{-i}, have infinite impulse responses. A particular choice of such a basis follows through the use of *orthonormal basis functions* (OBFs), which are specific basis functions in $\mathcal{H}_2$ (see [11]). Then an OBFs based LPV model structure is formulated as

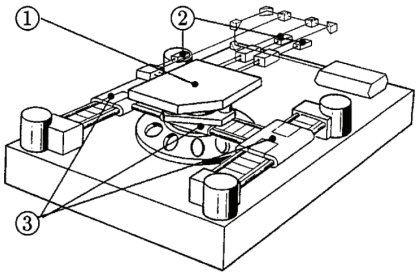

Fig. 1. Schematic view of the standard configuration of xy-positioning tables: (1) short stroke; (2) laser interferometers; (3) linear motors of the long and short strokes.

$$y(k) = W_0(p(k))u + \sum_{i=1}^{n} W_i(p(k))\phi_i(q)u, \qquad (6)$$

where $\{W_i\}_{i=0}^{n}$ are the p-dependent expansion coefficients of the truncated series expansion of $\mathcal{S}$ in terms of the OBFs $\{\phi_i\}_{i=1}^{n} \subset \mathcal{H}_2$ being analytic in the exterior of the complex unit disk. For a detailed overview of the properties of OBF based model structures like (6) and their identification approaches see [10]. Among many attractive properties of (6), it is worth to mention that unlike other IO type of model structures, OBF model structures have a direct LFR realization. In the sequel we will focus on the so called local type of identification of (6) by demonstrating its efficiency w.r.t. the data-driven modeling of an xy-positioning table. However, before that, let's investigate how such high-performance positioning devices can be modeled in the LPV framework based on first principle laws, why data-driven modeling is attractive for these systems and what are the expectations w.r.t. the produced models.

III. LPV MODELING OF xy-POSITIONING TABLES

xy-positioning tables are part of high-performance positioning devices used commonly in the production of *integrated circuits* (ICs). The conventional design of these devices, depicted in Fig. 1, involves a *long stroke*, called the xy-positioning table, moved by two linear motors on parallel rails. On the long stroke a third linear motor positions the *short stroke* which is magnetically levitated by a set Lorentz motors to achieve high accuracy positioning. The overall device is controlled in six motion *degrees of freedom* (DOFs) (3 translational and 3 rotational freedom), with usual servo error requirements in the order of $[1, 50]$ [nm]. However, the long stroke itself is often only controlled in the x, y-translational and the z-rotational DOF's. Besides the high accuracy requirements, high throughput is also a primary objective, giving rise to fairly aggressive motion parameters, with speeds in the order of $0.5 - 1$ [m/s] and accelerations in the order of $10 - 30$ [m/s^2].

A. First-principle modeling

The first-principle modeling concept of a conventional xy-positioning table is described in Fig. 2. In this modeling concept, it is assumed that the long stroke has no displacement in the x-direction, i.e. $x_2 = 0$. Under this assumption, the dynamical behavior of this multiple mass-damper-spring

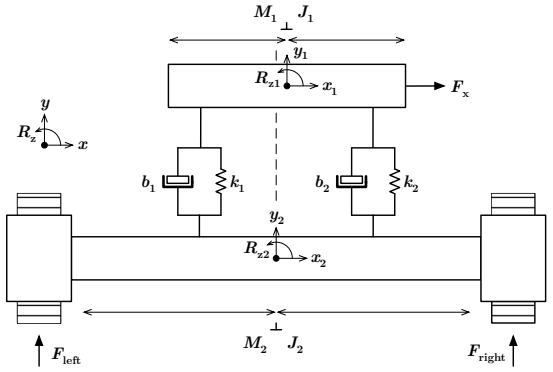

Fig. 2. First-principle modeling concept of xy-positioning tables.

system $\mathcal{S}$ can be described via the following differential equation:

$$r_{\mathrm{M}}\ddot{w} + r_{\mathrm{B}}(x_1)\dot{w} + r_{\mathrm{K}}(x_1)w = r_{\mathrm{F}}u \qquad (7)$$

where $w = [\ x_1 \quad y_1 \quad R_{\mathrm{z}1} \quad y_2 \quad R_{\mathrm{z}2}\ ]^\top$, $u = [\ F_{\mathrm{x}} \quad F_{\mathrm{left}} \quad F_{\mathrm{right}}\ ]^\top$ and r_{M} and r_{F} are full rank block diagonal matrices with appropriate dimensions and r_{B} and r_{K} are linear matrix functions of x_1. By taking $p = x_1$ as a scheduling variable with $\mathbb{P} = [\mathrm{x}_{\min}, \mathrm{x}_{\max}] \subset \mathbb{R}$, the differential equation (7) has a minimal continuous-time LPV-SS realization with input-output partition $([x_1\ y_1\ R_{\mathrm{z}1}], u)$ as

$$\mathfrak{R}_{\mathrm{SS}}(\mathcal{S}) = \left[\begin{array}{cc|c} 0 & I & 0 \\ -r_{\mathrm{M}}^{-1}r_{\mathrm{K}}(p) & -r_{\mathrm{M}}^{-1}r_{\mathrm{B}}(p) & -r_{\mathrm{M}}^{-1} - r_{\mathrm{F}} \\ \hline I & 0 & 0 \end{array}\right] \qquad (8)$$

Note that such an LPV model is called a quasi-LPV model as p is not an external variable of the system, however with a certain degree of conservatism this does not prevent the use of LPV control.

In the obtained MIMO-LPV model (8), forces in one direction have influence on the movements in other directions. More specifically, either of the forces F_{left} and F_{right} affect both the y-translation and the R_{z}-rotation. In particular, if $x_1 \neq 0$, then $F_{\mathrm{left}} = F_{\mathrm{right}}$ do not result in a pure y-movement, but also causes a rotation, since the end effector mass M_1 is felt differently by actuators F_{left} and F_{right}. Thus, to enable the design of SISO controllers the plant dynamics are commonly decoupled in practice by using pre- and post-transformation matrices T_{u} and T_{y} implemented directly into the hardware. As in the LPV case full decoupling of the IO channels is currently not a well-understood concept, thus the decoupling of the plant is developed by using a rigid-body formulation of (7), providing approximately decoupled dynamics (i.e. approximately diagonal) in the low-frequency region.

Based upon the above given considerations, the rigid-body decoupled plant can be written as:

$$\mathfrak{R}'_{\mathrm{SS}}(\mathcal{S}) = T_{\mathrm{y}}(p) * \mathfrak{R}_{\mathrm{SS}}(\mathcal{S}) * T_{\mathrm{u}}(p), \qquad (9)$$

where $\mathfrak{R}_{\mathrm{SS}}(\mathcal{S})$ is the LPV representation (8) of the plant dynamics. The matrix T_{y} is defined by the variables to be controlled: $y'_1 = y_1 - R_{\mathrm{z}1}x_1$ and $y'_2 = R_{\mathrm{z}1}$ which are the actual measurements available from xy-positioning tables (besides the measurement of x_1). Next T_{u} is developed

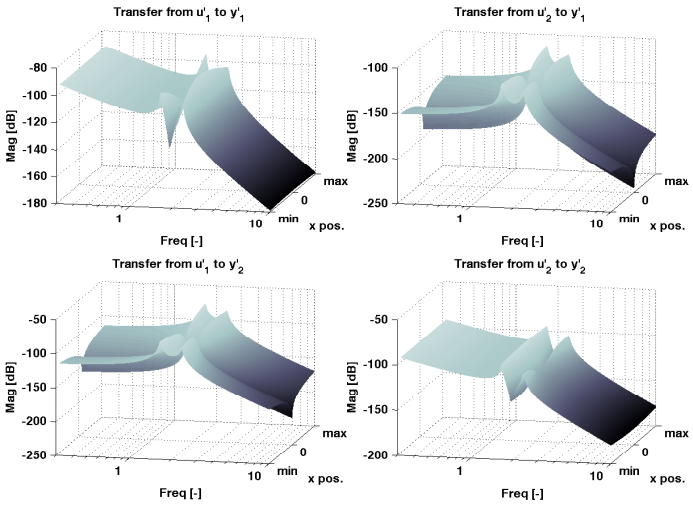

Fig. 3. Bode magnitude plot of the 2×2 MIMO xy-table model at different x-positions (in open-loop).

by assuming arbitrary slow variation of x_1 and aiming for $T_{\mathrm{u}}P_0T_{\mathrm{y}} = I$ where P_0 is the static gain of the system. By applying T_{y} and T_{u} in terms of (9) on the full model results in the following LPV-SS form:

$$\mathfrak{R}_{\mathrm{SS}}(\mathcal{S}') = \begin{bmatrix} A(p) & BT_{\mathrm{u}}(p) \\ T_{\mathrm{y}}(p)C & 0 \end{bmatrix} = \begin{bmatrix} A(p) & B'(p) \\ C'(p) & 0 \end{bmatrix} \quad (10)$$

In the sequel we will restrict our attention to the dynamical behavior of (10) w.r.t. output channels $y' = [\ y_1 - R_{\mathrm{z}1}x_1 \quad R_{\mathrm{z}1}]^\top$ and input channels $[\ F_{\mathrm{x}} \quad F_{\mathrm{left}} \quad F_{\mathrm{right}}\ ]^\top = T_{\mathrm{u}}(p)u'$. For these IO channels, the frozen FRF's of the first-principle model of a real-life xy-positioning table, obtained with the same modeling concept as (10), are depicted at different x_1-positions in terms of Bode magnitude plots in Fig. 3. To protect the interest of the manufacturer, frequency and time have been scaled throughout this paper. The following observations are crucial:

- The system dynamics can be clearly separated into an unstable rigid body part dominant in the low frequency band (below 1) and a x_1-position dependent stable flexible part dominant in the frequency band $[1, 3]$ which is symmetric in magnitude to the $x_1 = 0$ position (phase has a 180° drop at $x_1 = 0$ due to sign change).
- In the diagonal channels, rigid body dynamics correspond to a second order integrator, while in the off-diagonal channels, due to the decoupling, only a small proportional term can be observed.
- At $x_1 = 0$, the off-diagonal transfer functions become aprox. zero, indicating perfect decoupling. The order of the transfer functions corresponding to the diagonal channels (each with order 6) also drops by 2 at $p = 0$.

B. Expectations of modeling

Deriving first-principle models of more complicated xy-positioning table designs is commonly a rigorous and costly process often resulting in an inadequate accuracy of the model due to unmodeled dynamics relevant for the expected accuracy. The coefficients of the resulting model need to be estimated for each setup, requiring complicated measurement procedures. Such a modeling scheme is expected to be infeasible for next generation of lightweight structures. Thus it is important to derive efficient identification procedures which can provide accurate models of the dynamics based on measured data. However as a first step towards this aim, we will study the LPV identification of the previously developed first-principle LPV model (10) to be able to analyze the performance of the method w.r.t. the analytical form of the system. Expectation w.r.t. the aimed model are the following:

- High accuracy of the model w.r.t. both constant and varying trajectories of $p(t) = x_1(t)$. For constant values of p, the magnitude of the error in terms of the local or so called frozen *frequency response function* (FRF) of the system needs to be less than -40dB, while for varying trajectories of p the accuracy in terms of signal response needs to be at least in the magnitude of μm.
- Accurate modeling of rigid body dynamics.
- Effective low order modeling.

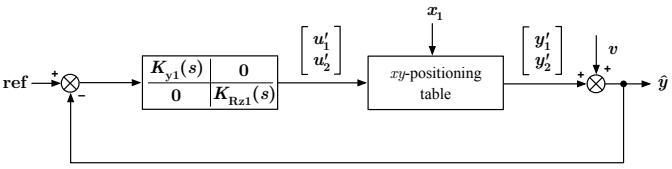

Fig. 4. Simplified closed-loop control scheme of the xy-table mechanism with measurement error v.

C. Simulation conditions

To setup a relevant simulation study where LPV identification of the considered xy-positioning table can be studied, it is important to simulate real-life conditions of experimentation. As the underlying system is unstable, therefore meaningful simulation or measurements can be taken only under closed loop control. For this purpose robust CT-LTI single-loop controllers $K_{\mathrm{y}1}(s)$ and $K_{\mathrm{Rz}1}(s)$ have been designed for the model satisfying moderate specs. in terms of performance. The complete closed control loop of the system is given in Fig. 4, which corresponds to a simplified control architecture used in practice.

In order to give a realistic setting for identification, noise affecting both the closed loop control and the data acquisition is also considered in the following form:

$$\hat{y}_1(k) = y'_1(k) + v_1(k), \quad \hat{y}_2(k) = y'_2(k) + v_2(k), \quad (11)$$

with v_1 and v_2 independent withe noise processes with normal distributions: $v_1(k) \in \mathcal{N}(0, \frac{1}{3}\cdot 10^{-7})$ and $v_2(k) \in \mathcal{N}(0, \frac{5}{3}\cdot 10^{-6})$. Such levels of noise are typical under the considered laser-interferometers based high-accuracy position measurements. Note that these noise conditions seem to be not so significant, but due to the relatively small range of movement and the tight error specifications we will see that they are challenging enough. Additionally, to record DT data for identification purposes, the inputs and outputs of the xy-positioning table in Fig. 4 are sampled with a sampling frequency of 20 [-] (i.e. $10\times$ the highest interesting frequency

point: 2 [-]), which is adequate to model the high-frequency behavior of the system.

IV. OBFs BASED LPV IDENTIFICATION

In the LPV identification literature a wide variety of different identification approaches have been introduced (see [9], [10] for recent overviews). Methods available can be classified based on the used model structure or the type of applied identification paradigm: like global and local approaches. In case of *global approaches*, an LPV model is identified based on data records with varying p while in case of the *local approaches* first LTI models of the plant are identified around specific operating conditions (constant p) and then the resulting models are interpolated on $\mathbb{P}$ to form a global LPV model. Each paradigm has its advantages and weak points, however it is generally true that it is very difficult to include identification constraints into global methods which would guarantee a specified upper bound of the model accuracy for constant p (local fit). Moreover, LPV systems do not have a transfer function representation. Therefore, it is only possible to include frequency domain constraints for local type of approaches. Regarding the specification of the identification problem given in Sec. III-B, it becomes obvious that a local approach is attractive for the considered setting. Among local LPV identification approaches, OBFs based methods have certain advantages due to the fact that interpolation in terms of local snapshots of the coefficients of e.g. (6) is well-posed and not affected by problems observed for state-space model structures (see [12]). Additionally, the resulting LPV-OBF model has a direct LFR realization avoiding the complicated realization approaches required for input-output type of model structures. Due to these considerations, in the sequel an LPV local type of identification approach is introduced which aims to capture the behavior of (10) with the model structure (6) using an OE noise model. In order to guarantee the tight FRF specifications we will take a frequency-domain approach to accomplish the local identification steps. The relevant questions here are how to choose the basis functions $\{\phi_i\}_{i=1}^{n}$ to provide an efficient representation of the dynamics, how to estimate local snapshots of $W_i(p)$ to guarantee the specified FRF constraints, and how to provide interpolation such that the model fulfills the constraints between the interpolation points while its performance for varying p will also be acceptable.

A. Choice of model structure

Based on the observations in Sec. III-A, it is attractive to separate the system dynamics into an additive "rigid-body part," which is not dependent on p, and a remaining "flexible part" that contains the varying-poles related dynamical aspects of the system. By identifying the flexible part with a fixed DT rigid body filter provides the means to enforce the well-known fact that the low-frequency behavior of the system is governed by decoupled 2^{nd}-order integrators with an additional zero at -1 for each diagonal IO channel:

$$\phi_{\mathrm{R}}(z) = \frac{z+1}{(z-1)^2}. \tag{12}$$

It can also be observed in Fig. 3 that the "moving" pole locations of the underlaying IO channels of the system are the same. This implies that the optimal set of OBFs, which provide the fastest convergence rate, is the same for each channel. Furthermore, local approaches can only identify coefficients, like W_i in (6), with static dependence. Thus the overall model structure can be chosen as

$$\hat{y}_\theta = \begin{bmatrix} c_1\phi_{\mathrm{R}}(q) & 0 \\ 0 & c_2\phi_{\mathrm{R}}(q) \end{bmatrix} u + \sum_{i=1}^{n_{\mathrm{g}}} W_i(p)\phi_i(q)u \tag{13}$$

where $\{\phi_i(q)\}_1^{n_{\mathrm{g}}}$ is a set of SISO OBF's and $c_1, c_2 \in \mathbb{R}$ with $W_i : \mathbb{P} \to \mathbb{R}^{2\times 2}$ are the unknown coefficients to be estimated which are specific w.r.t. the underlaying system. The next question is how to obtain basis functions that guarantee a fast convergence rate of (13) w.r.t. the considered system. However, before that it is important to design our experiments which will give the information upon which adequate selection of the basis functions and the estimation of the expansion coefficients will be accomplished.

B. Experiment design & data generation

The first step of experiment design for local identification is the gridding of $\mathbb{P}$. This refers to designing the points on the x_1-axis around which local LTI identification of the setup will be performed. It is important that the gridding must be dense enough to capture important dynamic changes of the plant for different x_1-positions. By analyzing the rate of change of the frozen poles and zeros of the system w.r.t. $\mathbb{P} = [\mathrm{x}_{\min}, \mathrm{x}_{\max}]$, a grid of 21 equidistant points is chosen.

In order to generate informative data for frequency-domain identification at the designated x_1-positions, orthogonal multisines with normalized amplitude are generated based on 2^{14} equidistant frequency points $\mathcal{W} = \{\omega_k\}_{k=1}^{2^{14}}$ in the range $[10^{-4}, 10]$. This frequency range has been chosen to contain the relevant dynamical aspect of the plant in terms of rigid body and flexible modes. The orthogonality of the generated multisine signals $r_{11}, r_{12}, r_{21}, r_{22}$ can be understood in the following manner: the *discrete-time Fourier transforms* $R_{11}(\omega), \ldots, R_{22}(\omega)$ of these signals, satisfy that

$$R(\omega_k)R^{\mathrm{H}}(\omega_k) = \begin{bmatrix} \lambda_1(\omega_k) & 0 \\ 0 & \lambda_2(\omega_k) \end{bmatrix} \prec I, \quad \omega_k \in \mathcal{W},$$

$$\text{where} \quad R(\omega_k) = \begin{bmatrix} R_{11}(\omega_k) & R_{12}(\omega_k) \\ R_{21}(\omega_k) & R_{22}(\omega_k) \end{bmatrix}.$$

This property ensures high accuracy frequency domain estimates in closed loop even under heavy measurement noise.

In the experiments first signals r_{11} and r_{21} are used as references for $y_1 - R_{\mathrm{z}1}x_1$ and $R_{\mathrm{z}1}$ (see Fig. 4) and with constant x_1 equal to a grid point. Then the whole experiment is repeated by using r_{12} and r_{22}. The two set of responses for $y_1 - R_{\mathrm{z}1}x_1$and $R_{\mathrm{z}1}$ are required to uniquely estimate the 2x2 MIMO FRF of the plant at the considered x_1 position. Note that the normalized reference signals are multiplied with 10^{-4} to remain in the operating range of the setup.

With the designed multisine sequence, data is generated based on the closed loop model starting from zero initial conditions. To generate an appropriately long data record

for the attenuation of both the transient and noise effects, the designed multisines are repeated 25 times. For validation purposes noise free data records are also generated.

C. FRF estimate of the local behaviors

The data records that are collected in the previous step now can be used to deliver estimates of the FRF of the system at the chosen x-positions. Consider the data sets $\mathcal{D}_{\mathrm{p},1} = \{y'_{\mathrm{ref}1}(k), u'_{\mathrm{ref}1}(k), r_{\mathrm{ref}1}(k)\}_{k=1}^{N_\mathrm{d}}$, $\mathcal{D}_{\mathrm{p},2} = \{y'_{\mathrm{ref}2}(k), u'_{\mathrm{ref}2}(k), r_{\mathrm{ref}2}(k)\}_{k=1}^{N_\mathrm{d}}$ where $T_\mathrm{u}(\mathrm{p})u'_{\mathrm{ref}i} = \begin{bmatrix} F_\mathrm{x} & F_\mathrm{left} & F_\mathrm{right} \end{bmatrix}^\top$ and $y'_{\mathrm{ref}i} = \begin{bmatrix} y_1 - R_\mathrm{z}x_1 & R_{\mathrm{z}1} \end{bmatrix}^\top$ collected from the model with $x_1 = \mathrm{p}$ and reference signals $r_{\mathrm{ref}i} = \begin{bmatrix} r_{1i} & r_{2i} \end{bmatrix}^\top$. Denote the *fast Fourier transform* (FFT) of these signals taken on one period of the time-domain data as $R_{\mathrm{ref}1}(\omega)$, $U'_{\mathrm{ref}1}(\omega)$, $Y'_{\mathrm{ref}1}(\omega)$ and $R_{\mathrm{ref}2}(\omega)$, $U_{\mathrm{ref}'2}(\omega)$, $Y'_{\mathrm{ref}2}(\omega)$ respectively. Due to the periodic nature of the excitation, it is true that after the transients have died out the FFT of each period of the measured data records only differ from each other in terms of the additive noise. Therefore, by chopping off the transient part of the data records (first 5-10 periods) and averaging the results of the FFT on the remaining periods, the effect of the noise can be averaged out. Thus in the sequel consider these spectra as the averaged FFT of the non-transient periods. Let

$$\begin{aligned}
\bar{U}(\omega) &= \begin{bmatrix} U'_{\mathrm{ref}1}(\omega) & U'_{\mathrm{ref}2}(\omega) \end{bmatrix}, \\
\bar{Y}(\omega) &= \begin{bmatrix} Y'_{\mathrm{ref}1}(\omega) & Y'_{\mathrm{ref}2}(\omega) \end{bmatrix}, \\
\bar{R}(\omega) &= \begin{bmatrix} R_{\mathrm{ref}1}(\omega) & R_{\mathrm{ref}2}(\omega) \end{bmatrix},
\end{aligned}$$

The classical way to estimate the FRF of the plant for a given frequency point $\omega_k \in \mathcal{W}$ is

$$\hat{F}(\omega_k) = \bar{Y}(\omega_k) \cdot \bar{U}^{-1}(\omega_k). \tag{14}$$

However, it is well known that such an empirical transfer function estimate is biased in case of closed-loop data. To have an unbiased estimate is better to consider

$$\hat{F}(\omega_k) = \left(\bar{Y}(\omega_k)\bar{R}^\mathrm{H}(\omega_k)\right) \cdot \left(\bar{U}(\omega_k)\bar{R}^\mathrm{H}(\omega_k)\right)^{-1}. \tag{15}$$

Among many choices of unbiased closed loop estimators, (15) has also been observed in the literature to deliver good results under heavy noise settings [13].

By using the data records and the estimation approach (15), FRF estimates of the plant at the considered scheduling points have been calculated. During the calculation the first 10 periods in the records have been removed to attenuate the effect of initial conditions. The results at position x_min are depicted in Fig. 5. From this figure it is obvious that the method delivers almost perfect estimate of the frozen FRFs on each IO channel. Furthermore the considered noise only significantly affects the high-frequency band beyond the flexible modes, which provides that accurate frequency-domain information is available to recover the most important dynamical aspects of the plant form measured data.

D. Selection of the OBF filter banks

To arrive at an adequate selection of the OBF functions in (6) the so called Fuzzy-Kolmogorov c-Max (FKcM) approach provides a practically applicable solution [14]. This approach uses a clustering type mechanism to assign a set

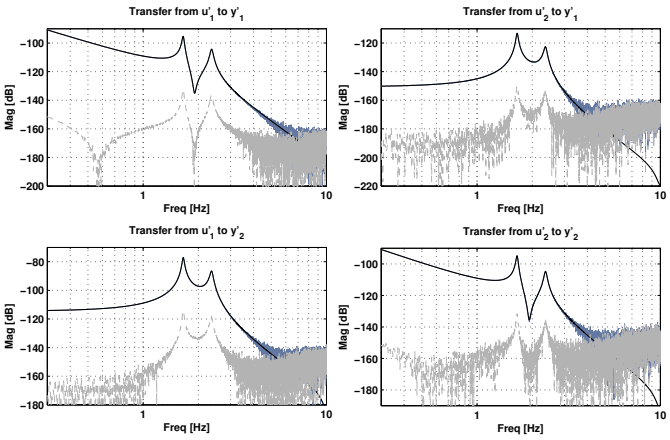

Fig. 5. Bode magnitude plot of the estimated FRF of the plant at position x_min. Original plant (black), estimated FRF (grey), error (light grey).

of basis functions w.r.t. observed frozen pole locations of an LPV system, such that these functions have the least worst-case expansion error. The expansion error is considered in terms of the so called *Kolmogorov n-width cost*: worst-case $\mathcal{H}_2$ error w.r.t. all possible transfer functions which have the observed pole locations. See [14] for a detailed description of this algorithm. The fuzziness variable m of this algorithm provides a trade off between computational complexity (small if $m \gtrsim 1$) and optimality of the solution ($m \to \infty$).

To obtain an estimate of the frozen pole locations of the xy-positioning table model at the considered x-positions a general *curve fitting* method can be applied on the previously obtained FRF estimates. Here the approach of the FREQID toolbox has been used [15]. To arrive at the correct number of poles a MIMO common denominator model with 8^th order has been estimated with curve fitting. The worst-case absolute error of the resulting pole estimates w.r.t. the true pole locations of the system at the given x-positions is 0.007%.

Next the FKcM approach is applied on the obtained highly-accurate pole estimates. By analyzing the results of the algorithm based on the estimated pole locations it has been observed that nearly optimal basis selection can be achieved if the fuzziness m is set to 35. Using this fuzziness value the algorithm has been executed on the estimated pole locations. The algorithm has been used with different number of optimized basis functions n_g and the results are summarized in Table I. In this table, as a performance measure, the Kolmogorov n-width cost (see before) has been computed in dB both for the obtained pole estimates and also for all true frozen pole locations of the xy-positioning table in the considered x-region. From Table I it follows that the obtained OBF poles achieve very small representation error w.r.t the estimated poles (small Kolmogorov cost). However, w.r.t. the true pole locations a dramatic difference can be observed between the set of 4 or 16 basis functions. Further analysis of the results, which is not described here due to space limitations, shows that at least 12 basis functions are needed to represent adequately the varying system dynamics on $\mathbb{P}$. After posteriori assessment of estimation with 12 and

TABLE I

ACHIEVED KOLMOGOROV n-WIDTH COST BY THE FKcM PROVIDED OBF'S FOR FUZZINESS $m = 35$ AND DIFFERENT NUMBER OF OBFS n_{g}.

n_{g}	estimated frozen poles	true frozen poles
4	-61.061 dB	-1.651 dB
8	-125.884 dB	-7.084 dB
12	-197.604 dB	-12.03 dB
16	-257.905 dB	-16.845 dB

16 basis functions it is concluded that 16 basis functions are required to meet with the aimed specifications. It can also be shown that beyond 16 basis functions the improvement in model accuracy is not significant. Thus in the sequel, we will consider the OBF set with 16 basis functions selected by the FKcM approach to formulate (13).

E. Estimation of the expansion coefficient dependence

By having the OBF filter banks chosen, the last remaining step of identification is to estimate the constants c_1, c_2 and the expansion coefficients $W_i(p)$ in (13). For this purpose the already calculated FRF estimates of the system are used. Note that the frequency response of the OBF filters and the first-principles suggested rigid body filters can be computed w.r.t. the frequency points of the FRF estimate and in terms of the model structure these frequency responses should approximate the estimated FRFs by linear combination. Thus, estimation of the samples of the expansion coefficients W_i at each considered grid point $\mathrm{p} \in \mathcal{P}$ reduces to a simple linear regression. After solving the linear regression the resulting samples of each W_i can be interpolated using any approach like polynomial, spline, Chebysev, etc. After investigation of the obtained results with each method, it have been concluded that a polynomial interpolation provides the most efficient solution in terms of the complexity/accuracy trade off. Regarding polynomial interpolation it has been concluded that for the case of 16 OBF functions a polynomial order of 15 is minimally required to achieve a good approximation of the frozen dynamics. By using the FRF estimates the samples of the expansion coefficients of the OBF filter banks obtained in the previous section with $n_{\mathrm{g}} = 16$ have been estimated and these samples have been interpolated with 17^{th} order polynomials. The results are depicted in Fig. 6. These figures show that using only a few estimated samples of the coefficient functions a close approximation of the polynomial dependencies can be obtained. This concludes the identification as the delivered model now can be explicitly realized in an LFR form.

V. VALIDATION OF THE MODEL

As a final step it remains to validate the obtained model in both the frequency and the time domain.

A. Frequency-domain validation

The obtained LPV-OBF model can be compared in terms of its frozen frequency responses to the behavior of the first-principle model. For the OBF model with 16 basis functions and 17^{th}-order polynomial dependence, the frozen frequency responses for each IO channel has been computed on a fine grid $\mathcal{P} \subset \mathbb{P}$ together with the response of the true system

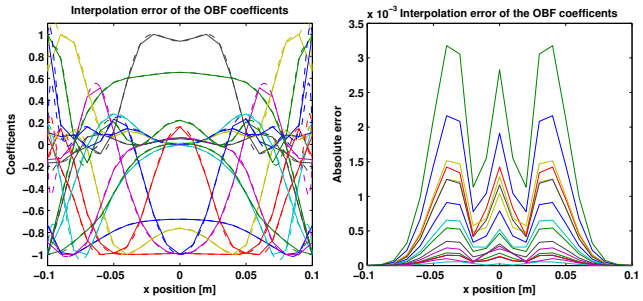

Fig. 6. Optimal coefficient functions W_i of the OBF's $n_{\mathrm{g}} = 16$ (solid lines) w.r.t. the frozen transfer functions between y_1 and u_1 at the grid positions x_1 together with their polynomial approximation (dashed lines).

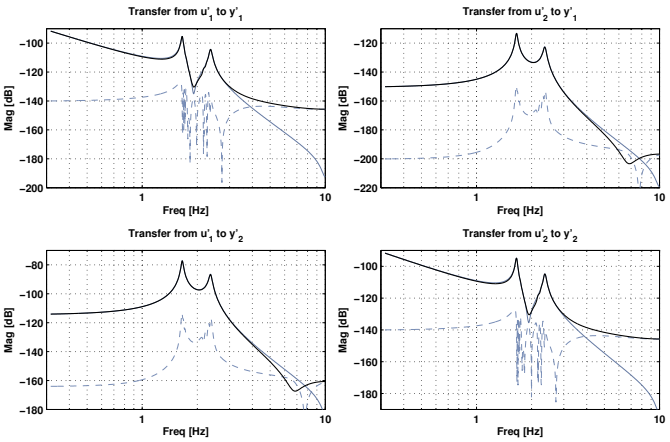

Fig. 7. Bode magnitude plot of the frozen frequency response at position $\mathrm{x}_{\min}$ of the estimated LPV-OBF model obtained with 16 basis functions and 17^{th}-order polynomial coefficient dependence. Original plant (black), estimated OBF model (grey), approximation error (dashed grey).

and visualized in terms of Bode plots. The results at $\mathrm{x}_{\min}$ are given in Fig. 7 which corresponds to the worst-case model fit. By analyzing these results the following observations can be made:

- The overall difference between the magnitude error and magnitude of the transfer functions is aprox. 40 dB.
- However, the error increases with an aprox. 20 dB around the anti-resonance mode. This results as a side effect of linear regression. Using better tuned weights this error can be decreased if necessary.

This means that specifications in terms of frequency-domain accuracy could be achieved with the investigated identification approach.

B. Time-domain validation

It is also important to investigate the time-domain behavior of the identified LPV-OBF model. First the open-loop response of the model is computed by using recorded u and p signals from a closed-loop simulation of the original xy-positioning table model for a monotone increasing p which corresponds to a fast sweep over $\mathbb{P}$. The used reference signals here are 0 set-point for $R_{\mathrm{z}1}$ and a typical step-like pattern for y_1, designed in terms of optimal speed, acceleration and jerk profile. The resulting responses of the LPV-OBF model (after re-transformation with $T_{\mathrm{y}}(p)$) are given in gray in Fig. 8 while the response of the original plant is given in black. The error is dominated by a small

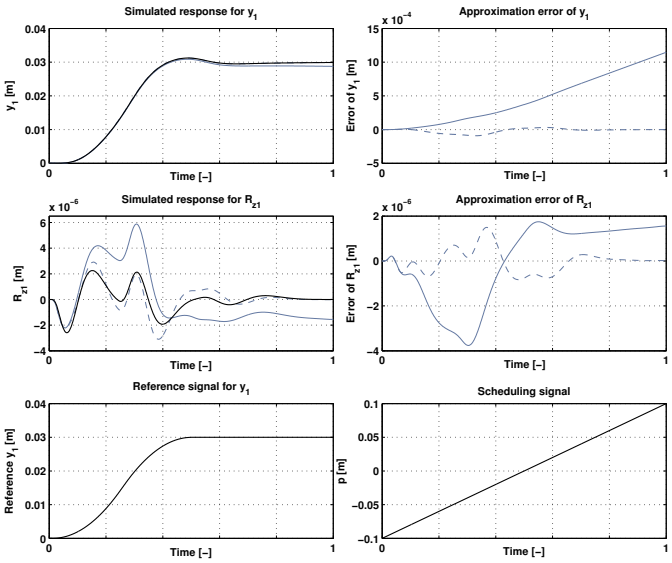

Fig. 8. Time-domain validation of the estimated LPV-OBF model using 16-basis functions with 17^{th}-order polynomial coefficient dependence. Simulated closed-loop response of the original plant is given with black for the reference and scheduling signals depicted in the lower two figures. The simulated response of the OBF model based on the closed loop input signals of the plant is given with grey (open-loop validation) while the closed-loop response of the model for the given reference signal is depicted with dashed grey (closed-loop validation).

difference that looks like the step response of an integrator. This yields that the identified LPV-OBF model is capable to reproduce the response of the system with high accuracy and the main source of the error is related to small differences between the unstable part of system and the LPV-OBF model. This hypothesis is also validated by the closed-loop response of the LPV-OBF model given with dashed gray in Fig. 8. It is important to note that validation of the model for varying p is rather unfair expectation for the LPV-OBF model as it was obtained purely on the basis of the frozen behavior of the system. By achieving an acceptable error which meets the aimed specs. we can finally conclude that the proposed identification approach can deliver high-quality model estimates.

C. Economical size

As we could see, a high number of OBFs and a high-order polynomial coefficient dependence have been needed to capture the dynamics of the xy-table with the desired accuracy. This means that the final LFR form of the identified model (13) is relatively large with $\dim(x) = 4 + 2 \cdot 16 = 36$ and $\dim(z) = 2 \cdot 17 = 34$. However, by applying recent methods in LPV model reduction, like the approach of [16], this LFR form can be reduced to state dimension 8 and with a $\dim(z) = 5$, without a significant loss of accuracy (the results are not presented here due to space restrictions). The explanation lays in the fact that in the considered model structure (13) all dependencies on p are at the output-side. Therefore in terms of realization there is a certain freedom to consider states and input contributions which also depend on p and hence can reduce the total dimension of the model.

VI. CONCLUSIONS

In this paper the identification of a xy-positioning table high-performance positioning system has been studied in the linear parameter-varying (LPV) framework. It has been shown that a local type of LPV identification approach based on orthonormal basis functions (OBFs) can deliver a high-accuracy estimate of the system both in terms of frozen frequency-domain and global time-domain accuracy. The applied frequency-domain approach has been essential to meet with the desired accuracy of the model and to suppress the effect of measurement noise, while the OBFs based structure provided a well-posed interpolation for the estimated frozen frequency response functions of the system.

REFERENCES

[1] M. Steinbuch and M. L. Norg, "Advanced motion control: An industrial perspective," *European Journal of Control*, vol. 4, pp. 278–293, 1998.

[2] Y. Chait, M. Steinbuch, and M. S. Park, "Robust control of a high performance flexible electro-mechanical system." in *Structural dynamic systems computational techniques and optimization: Dynamic analysis and control techniques*, T. C. Leondes, Ed. London: Gordon and Breach, 1999, pp. 211–240.

[3] B. J. Kang, L. S. Hung, S. K. Kuo, S. C. Lin, and C. M. Liaw, "$\mathcal{H}_\infty$ 2DOF control for the motion of a magnetic suspension positioning stage driven by inverter-fed linear motor," *Mechatronics*, vol. 13, no. 7, pp. 677–696, 2003.

[4] M. van de Wal, G. van Baars, F. Sperling, and O. Bosgra, "Multivariable $\mathcal{H}_\infty/\mu$ feedback control design for high-precision wafer stage motion," *Control Engineering Practice*, vol. 10, no. 7, pp. 739–755, 2002.

[5] W. Rugh and J. S. Shamma, "Research on gain scheduling," *Automatica*, vol. 36, no. 10, pp. 1401–1425, 2000.

[6] K. Zhou and J. C. Doyle, *Essentials of Robust Control*. Prentice-Hall, 1998.

[7] C. W. Scherer, "Mixed $\mathcal{H}_2/\mathcal{H}_\infty$ control for time-varying and linear parametrically-varying systems," *Int. Journal of Robust and Nonlinear Control*, vol. 6, no. 9-10, pp. 929–952, 1996.

[8] M. G. Wassink, M. van de Wal, C. W. Scherer, and O. Bosgra, "LPV control for a wafer stage: Beyond the theoretical solution," *Control Engineering Practice*, vol. 13, no. 2, pp. 231–245, 2004.

[9] F. Casella and M. Lovera, "LPV/LFT modelling and identification: overview, synergies and a case study," in *IEEE International Symposium on Computer-Aided Control System Design*, San Antonio, Texas, USA, Sept. 2008, pp. 852–857.

[10] R. Tóth, *Modeling and Identification of Linear Parameter-Varying Systems*, ser. Lecture Notes in Control and Information Sciences, Vol. 403. Springer-Germany, 2010.

[11] P. S. C. Heuberger, P. M. J. Van den Hof, and Bo Wahlberg, *Modeling and Identification with Rational Orthonormal Basis Functions*. Springer-Verlag, 2005.

[12] R. Tóth, F. Felici, P. S. C. Heuberger, and P. M. J. Van den Hof, "Discrete time LPV I/O and state space representations, differences of behavior and pitfalls of interpolation," in *Proc. of the European Control Conf.*, Kos, Greece, July 2007, pp. 5418–5425.

[13] E. Wernholt and S. Gunnarsson, "Analysis of methods for multivariable frequency response function estimation in closed loop," in *Proc. of the 46th Conference on Decision and Control*, no. 3, New Orleans, Louisiana, USA, Dec. 2007, pp. 4881–4888.

[14] R. Tóth, P. S. C. Heuberger, and P. M. J. Van den Hof, "Asymptotically optimal orthonormal basis functions for LPV system identification," *Automatica*, vol. 45, no. 6, pp. 1359–1370, 2009.

[15] R. A. de Callafon and P. M. J. Van den Hof, "FREQID - frequency domain identification toolbox for use with Matlab," *Selected Topics in Identification, Modeling and Control*, vol. 9, pp. 129–134, 1996.

[16] D. Petersson and J. Löfberg, "Optimization based LPV-approximation of multiple model systems," in *Proc. of the European Control Conf.*, Budapest, Hungary, Aug. 2009, pp. 3172–3177.